ELSEVIER

Biophysical Chemistry 55 (1995) 261–271

Biophysical Chemistry

Influence of dynamic fluctuations on DNA curvature

P. De Santis *, M. Fuà, A. Palleschi, M. Savino

Dipartimento di Chimica and Fondazione Cenci Bolognetti — Istituto Pasteur, Dipartimento di Genetica e Biologia Molecolare, Università di Roma 'La Sapienza', Rome, Italy

Received 28 September 1994; revised 20 December 1994; accepted 31 January 1995

Abstract

The effect of dynamic fluctuations on physical manifestations of DNA curvature such as electrophoretic retardation, circularization of DNA tracts and nucleosomes positioning is examined. It is shown that in all cases the main features of the processes can be satisfactorily explained by a static curvature model, which appears to be a good representation of time and ensemble averaged superstructures of DNA chains. The dynamic fluctuations around the average curvature appear to influence only the kinetics of these processes.

In the case of polyacrylamide gel electrophoretic retardation it is demonstrated that the approximation of the static model holds on the assumption that dynamic fluctuations are independent from intrinsic curvature.

The actual validity of the static model we proposed several years ago is satisfactorily demonstrated by the explanation and prediction of different experiments, such as cyclic permutation gel electrophoresis, differential DNAase I cleavage of cyclic versus linear DNA tracts and nucleosome positioning.

Keywords: DNA curvature; Dynamic fluctuation; Electrophoretic retardation

1. Introduction

The existence of intrinsic and induced curvatures in DNA is well documented by their electrophoretic manifestations and by electron microscopy visualization [1–10]. Theoretical and semi-empirical models have been proposed to predict the curvature of DNA tracts and have been found to be in satisfactory agreement with experimental data. These models are based on the assumption that sequence dependent bends or wedges phased along the double helix provide the main factors for DNA curvature.

Several years ago we proposed a theoretical model for predicting directly the intrinsic superstructure of DNA tracts as well as the superstructure induced by circularization or protein association from the sequence. This was done by integrating the slight deviations, we theoretically evaluated, from the canonical B-DNA structure of the different dinucleotide steps [10–15].

It was very convenient to adopt the local or differential curvature — given in modulus and phase — as a useful function to localize the curved tracts along the sequence and the corresponding groove amplitudes that are relevant for DNAase I and Topoisomerase I specific cleavage, as well as to compare the superstructural features of different DNAs. Using such a complex plane representation, which we called 'curvature diagram', it is possible to evaluate the curvature dispersion, which we found to be a good measure of the gel electrophoresis retarda-

* Corresponding author.

Elsevier Science B.V.
SSDI 0301-4622(95)00034-8

tion factor, and to visualize the curved regions of a DNA tract along the sequence.

Recently, however, Olson et al. [16] criticized such a static representation of the DNA curvature, maintaining that it had no relation with the actual superstructure of a DNA tract and challenging its ability to interpret its relevant physical and biological properties. Their conclusions were based on a study of the influence of dynamic fluctuations on the overall size and shape of curved tracts of DNA, carried out using a matrix generator and Monte Carlo methods.

Our approach to the problem is different. We present the intrinsic superstructural features of DNA tracts as static or ensemble average curvature functions, instead of adopting the usual conformational statistic parameters, namely the end to end distance and the principal components of the second moment tensor of the virtual bond segmental distribution along the chain.

We believe that our model is more suitable for investigating DNA differential curvatures and its experimental manifestations in DNA tracts up to a few hundred base pairs, these being the most interesting for molecular biology.

The approach used by Olson and al. can, however, be useful for longer DNA tracts where the use of statistical dimensions might be more appropriate.

In the present paper we show that the curvature diagram obtained with the static method represents the time or ensemble average (assuming ergodicity) over the dynamic fluctuations of a DNA tract.

2. Methods

Derivation of the relevant parameters representing the curvature of a DNA tract are reported in the Appendix.

Here we adopt such kind of representation to evaluate the influence of thermal fluctuations of the DNA chain on the experimental manifestations of the sequence dependent curvature.

Let $\mathrm{d}(s,t)$ be the deviation vector representing the departure from the canonical B-DNA structure of the local helical axis at the sequence position s and at a time instant t. This deviation vector depends on the dinucleotide step at position s and stochastically on the time. The integration of the deviation vectors to a recurrent turn of double helix along the sequence gives the sequence and time dependent local curvature, $c(n,t)$, assigned at the central position n of that turn. It represents the vectorial deviation of the helical axis of the double helix turn at the nth position with respect to that at the $(n-1)$th position. This can be done by using matrix transformations or, more conveniently, by considering the very small values of the deviations which characterize the different dinucleotide steps, by using the complex plane representation.

Thus,

$$c(n,t) = \sum_{n\text{th turn}} \mathrm{d}(s,t) \exp(2\pi is/\nu)$$

where the summation is carried over a turn of the double helix about the position n of the sequence and ν is the average period of B-DNA ($= 10.4$).

Let $\mathrm{d}(s,t)$ be divided in two contributions: $\mathrm{d}(s,t) = \mathrm{d}(s) + \delta(s,t)$, the first addend representing the static deviation (corresponding to the time average deviation) and the latter one the time or dynamic fluctuation of the deviation vector in terms of roll and tilt angles,

$$\begin{aligned} c(n,t) &= c(n) + \sum_{n\text{th turn}} \delta(s,t) \exp(2\pi is/\nu) \\ &= c(n) + \chi(n,t) \end{aligned}$$

where,

$$c(n) = \sum_{n\text{th turn}} \mathrm{d}(s) \exp(2\pi is/\nu)$$

is the static bend of the helical axis in modulus and phase at position n of the sequence, graphically represented by the curvature diagram, and $\chi(n,t)$ is the harmonic component of periodicity ν of the time fluctuation angles around the static curvature, the only component of the thermal perturbations that contributes to the curvature of the helical axis.

The last expression strictly holds in the case of harmonic dynamics; however, it is important to note that anharmonicity effects of the dynamic fluctuations of the roll and tilt angles may be implicitly taken into account by using average values instead of minimum energy values. These have been obtained by slightly varying the roll and tilt angles from the minimum energy values in order to optimize the

correlation of experimental data as will be shown below [18].

Thus, averaging over a time interval significantly greater than the fluctuation time (reasonably in the range of ps) we obtain this expression:

$$< c(n,t) > = c(n) \text{ and } < \chi(n,t) > = 0$$

Therefore the curvature diagram conveniently represents the time average or the ensemble average curvature.

As an example Fig. 1 illustrates the curvature diagram of a mitochondrial DNA tract of *Crithidia fasciculata* of 663 bp, where the loop region of about 200 bp, characterized by high curvature and constant phase, can be easily recognized. This region shows the presence of circular forms up to about 70% of the electron microscope patterns in spite of the dramatic experimental conditions [1–3,19].

We adopted the same complex plane representation to evaluate the integral curvature $C(n,t)$ which gives the bend angle between the first and the nth local helical axis in order to evaluate its dispersion, σ^2, corresponding to the mean square deviation along the sequence of the integral curvature with respect to its average value:

$$C(n,t) = C(n) + \sum_{s=1}^{n} \delta(s,t) \exp(2\pi is/\nu)$$

$$= C(n) + \Xi(n,t)$$

where $C(n) = \sum_{s=1}^{n} \mathrm{d}(s)\exp(2\pi is/\nu)$ is the static integral curvature.

$$\sigma^2(t) = < |C(n,t) - < C(n,t) > |^2 >$$

$$= < C(n,t)|C(n,t) > - | < C(n,t) > |^2$$

$$= \sigma^2 + \sigma_0^2(t) + 2\mathrm{Re} < C(n) | \Xi(n,t) >$$

$$- 2\mathrm{Re} < C(n) > | < \Xi(n,t) >$$

where:

$$\sigma^2 = < C(n)|C(n) > - | < C(n) > |^2$$

is the static curvature dispersion we introduced in previous papers, and

$$\sigma_0^2(t) = < \Xi(n,t)|\Xi(n,t) > - | < \Xi(n,t) > |^2$$

represents the curvature dispersion due to the dynamic fluctuations corresponding to the curvature

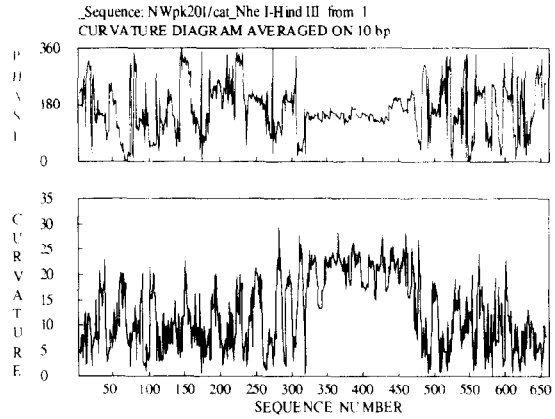

Fig. 1. Curvature diagram in modulus and phase of plasmid pk201 containing a mitochondrial DNA tract of 663 bp from *Crithidia fasciculata*. The modulus of the curvature at a given sequence number represents the bending of the helical axis per turn of B-DNA (in degrees). The complex phase represents the direction of the bending with respect to the pseudo dyad axes of the first bp oriented towards the large groove. A constant phase along a DNA tract indicates that the chain axis is planar, namely, that the double helix axis is coherently bent in the same direction.

dispersion of a canonical straight DNA tract (namely, a DNA with a random distribution of bases along the sequence). The integration is made over the sequence number n.

The time or the ensemble average is obtained by integrating the curvature over a time interval longer than the fluctuation time, t:

$$< \sigma^2(t) > = \sigma^2 + < \sigma_0^2(t) >$$

The time average of the last two terms of $< \sigma^2(t) >$ is zero in absence of a significant correlation between the dynamic fluctuations and curvature as assumed also by Olson et al. [16]

Also in this case $< \sigma^2(t) >$ could be, in principle, correctly calculated by using matrix transformations and the curvature diagram. In any case, the postulated independence of the dynamic fluctuations from the curvature, (namely from the sequence), results in a simple summation of the static and dynamic dispersions.

Therefore, $< \sigma_0^2(t) >$ represents the average of the stochastic curvature dispersion along DNA or the curvature dispersion of a DNA tract with random distribution of bases along the sequence.

We have previously shown that the polyacrylamide gel electrophoretic anomalies, experimentally found by different authors in natural and synthetic DNA tracts, are strictly related to their static curvature dispersion. In fact, we will demonstrate that, with a reasonable approximation, such anomalies are practically independent from dynamic fluctuations.

3. Polyacrylamide gel electrophoretic manifestations of curvature

Current theories on the gel electrophoresis mobility of linear DNA are based on the reptation model proposed by De Gennes [20] which was later developed by Lerman and Frisch, Lumpkin and Zimm and Levene and Zimm [21–23]. According to this model in which DNA is imagined to migrate in a snakelike fashion among the fibers of the gel. These constrain the translation of the chain along preferential pathways in the electric field direction. If a tight gel is used, the mobility of the chain is expected to involve elastic deformation free energy of the DNA chain moving around the obstacles in the gel network.

The reptation model correctly predicts the dependence at low fields of the electrophoretic mobility on the inverse of the length of DNA tracts. However, many DNA tracts of biological relevance as well as numerous sequential double helical multimeric oligonucleotides, with periodicity restricted in a narrow interval around the B-DNA helical period, show large electrophoretic anomalies since they behave like chains characterized by an apparent molecular weight higher than the real one. Such reduction of the electrophoretic mobility is quantified as retardation R corresponding to the ratio between the apparent and the actual base pair numbers and it is generally accepted to be a manifestation of the intrinsic superstructure of DNA.

By analyzing a large number of multimeric sequential oligomers, we have found that the electrophoretic retardation appears to be a function of the molecular weight and the modulus of the curvature as proved by the good correlation obtained between retardation and theoretically evaluated curvature for all the multimeric decanucleotides experimentally investigated by different authors.

The existence of a correlation between retardation and curvature prompted us to investigate the possible physical relations between these quantities. This problem is related to that of finding the mobility of a curved DNA relative to that of an equivalent straight DNA tract.

In fact, if the mobility of a DNA tract, 50–200 bp, is assumed to be proportional to the inverse of its length, the ratio between the mobilities of a straight and a curved DNA can be replaced by the ratio between the apparent length of the curved DNA and the actual length of the straight DNA. Thus, the electrophoretic retardation could be related with good approximation to the mobility ratio:

$$R = N_{\text{app.}}/N_{\text{act.}} = \mu_{\text{str.}}/\mu_{\text{cur.}}$$

As a consequence, if one adopts the simple thermodynamic hypothesis that the reduced mobility of curved DNA depends on the different activation energy required for travelling among the network of gel fibers in the electric field direction, the mobility ratio should be exponentially related to such activation energy difference, namely to the average straightening energy of the curved DNA in the direction of the average orientation of the helical axis

$$R = \exp(-\beta(E_{\text{str.}} - E_{\text{cur.}}))$$

Thus, retardation should be a manifestation of the longer relaxation time that curved DNA takes to reach a quasi-straight structure which should be more suitable for travelling among the gel fibers in the electric field direction [18].

Assuming a simple harmonic model of DNA deformation, the straightening activation energy comes out to be proportional to the angular dispersion of the local helical axes around their average value.

Thus, if

$$E_{\text{cur.}} = b < \sigma^2(t) > = b(\sigma^2 + < \sigma_0^2(t) >)$$

and

$$E_{\text{str.}} = b < \sigma_0^2(t) >$$

where b represents an apparent elastic force constant. Retardation can be thus expressed:

$$R = \exp(\beta b \sigma^2) \text{ or } \ln R = B\sigma^2$$

which for small curvatures can approximately be linearized to:

$$R = 1 + B\sigma^2$$

These are the expressions we proposed in previous papers [14,18]. Therefore, the retardation, which represents a normalized gel electrophoretic mobility relative to an equivalent straight DNA tract, appears to depend only on the static curvature dispersion because of the compensation of the dynamic fluctuations we assumed to be approximately equivalent in straight and curved DNA.

This approximation was also adopted by Olson et al. and appears to be justified by the experimental results.

$< \sigma_0^2(t) >$ can be evaluated using the generally accepted value of the DNA persistence length $P =$ 500 Å. It is equivalent to the gyration radius of a random walk on the unit sphere of the chain of the angular monomeric deviations, δ, from the straight B-DNA.

The statistical value of the persistence length is well known to be related for small angles to the squared average value of $\delta(n,t)$

$$P = 2r/ < \delta^2 >$$

where $r = 3.4$ Å, the monomeric repeat.

Therefore $< \delta^2 > = 6.8/P = 0.014$ rad^2 and assuming this value we obtain an approximated evaluation of the time averaged angle between the local helical axis of the last nucleotide with respect to the first one, $< \Xi^2(N) > = N < \delta^2 >$ assuming a random walk on the unit sphere. $< \sigma_0^2(t) >_t$ is the corresponding gyration radius, hence:

$$< \sigma_0^2(t) >_t = < \delta^2 > N/6 = 2Nr/6P = L/3P$$

where L is the contour length.

It must be noted that at high R, σ^2 shows increasing positive deviations, which suggests a possible negative correlation (we have neglected the term $\mathrm{Re} < C(n) | \Xi(n,t) >$ in the previous expression) between curvature and dynamic fluctuations.

In contrast to what was reported in the Olson et al. paper [16], our model reproduces with an adequate approximation the full trend of retardation versus molecular weight as illustrated in Fig. 2 in the case of the multimeric oligomer GA4 [6]; it consistently explains the progressive reduction of the gel electrophoretic anomalies in DNA tracts in presence of increasing concentration of intercalating drugs including the case of GC affinity [24]. The relevant twist changes induced by intercalation produce a loss

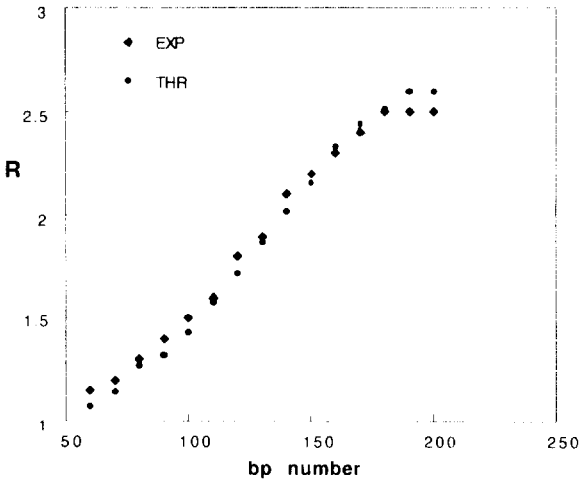

Fig. 2. Comparison between experimental and theoretical PAGE retardation values versus molecular weight for the Hagerman multimeric oligomer GA4 [6].

of the necessary coherence of the local curvature in the curved DNA tracts with the consequent reduction of the curvature dispersion.

It is interesting to note that the local deviation parameters we adopted, namely roll and tilt angles of the different dinucleotide steps, were in a first ap-

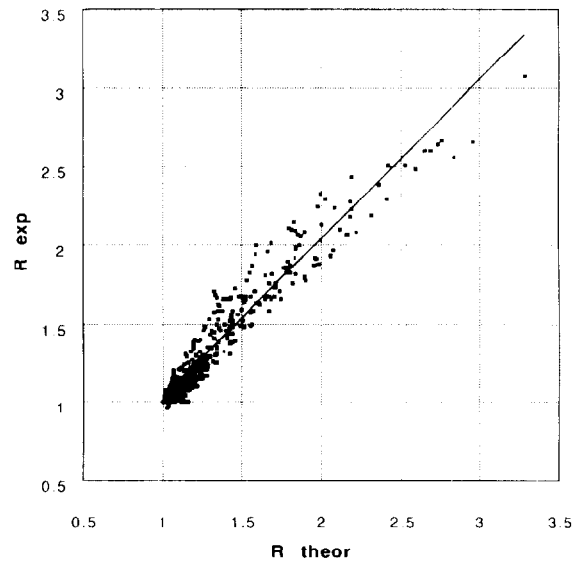

Fig. 3. Correlation diagram of theoretical and experimental PAGE retardation values of 450 multimeric oligomers differing in sequence, periodicity and molecular weight.

proximation obtained by using conformational energy calculations and were thereafter refined in order to obtain the best fitting of the electrophoretic data at room temperature of a large set of synthetic and natural DNA tracts. We have thus also implicitly taken into account some approximations of our model relative to both DNA curvature and gel electrophoresis retardation.

The correlation between theoretical and experimental values of PAGE retardation for a large ensemble of sequences is reported in Fig. 3.

It is worth to report that using this approach it is possible to reproduce satisfactorily the experimental features of two very stringent electrophoretic manifestations of DNA curvature, namely the influence of point mutations on the electrophoretic mobility of a SV40 DNA tract 173 bp and the cyclic permutation electrophoretic behavior of long DNA tracts, as reported in Figs. 4–6.

4. Role of the intrinsic curvature on the anisotropic flexibility of DNA

Because of the assumed low covariance between chain dynamics and curvature, the dynamic fluctuations appear to be independent from the sequence, although they influence the kinetics of the process when a DNA tract is constrained to assume a superstructure different from its intrinsic one by circularization or protein association such as in nucleosomes.

The pioneering experiment by Drew and Travers [25] on the differential digestion of the Tyr T DNA tract of 169 bp with DNAase I, has shown that DNA has an intrinsic propensity to deform anisotropically and coherently when it gives rise to either a circular or a nucleosomal form.

This suggested that the bendability of DNA could be a function of the intrinsic curvature. As a matter of fact, by adopting first order elasticity and our static model we have shown that the induced curvature is a function strictly related to the sequence dependent curvature by the principle of minimum square deviation: the results we obtained convincingly confirm the validity of the 'static model' in predicting the induced curvature.

We have in fact reproduced the main features of the experiment performed by Drew and Travers on the differential DNAase I cleavage of circular DNA with respect to the linear form and explained some

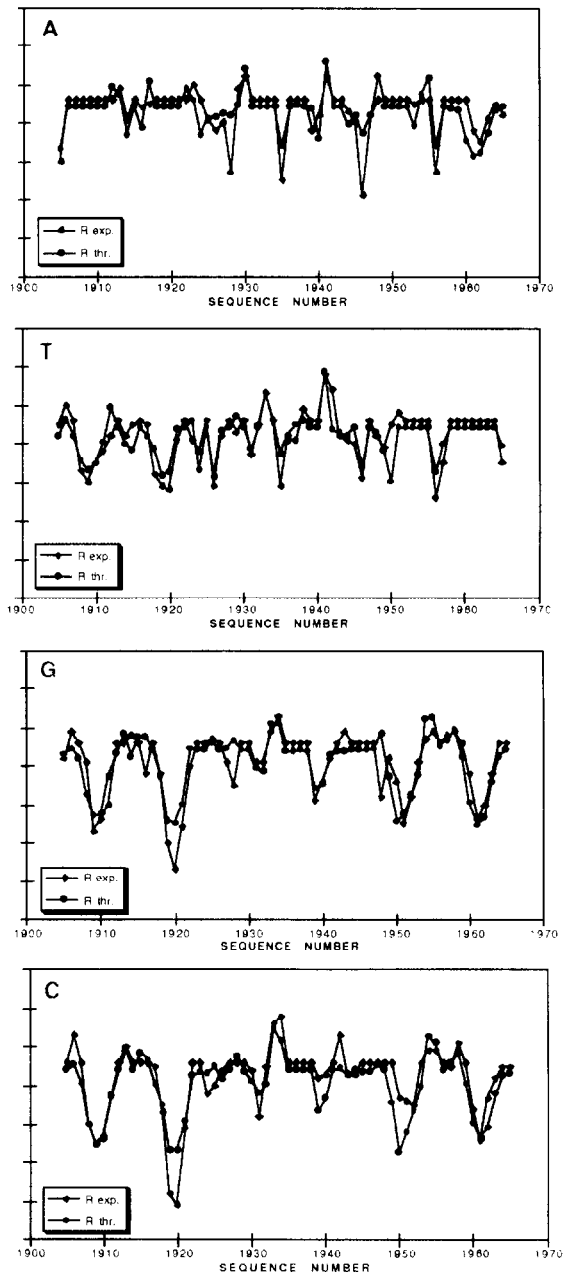

Fig. 4. Comparison between theoretical and experimental PAGE retardation trend of 195 point-mutated DNAs obtained by single base substitution from a SV40 tract of 173 bp long. The experimental data are those reported in Ref. [17].

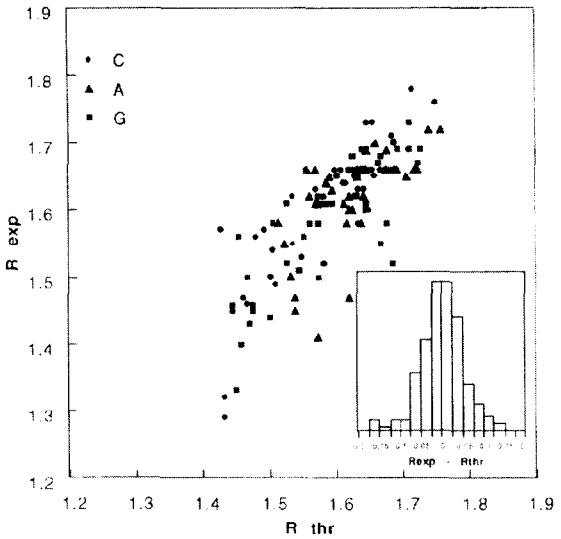

Fig. 5. Correlation diagram of theoretical and experimental values of retardation for the 195 point-mutated DNAs [17] and relative dispersion.

fine characteristics of the pattern of the cleavage probability by DNAase I. [15,26].

Adopting as a normalized distortion energy the ratio between the squared vectorial difference of the intrinsic and induced curvatures of recurrent DNA tracts of 145 bp, and the corresponding value of an equivalent tract but with randomized sequence, it has been possible to predict phasing and positioning of nucleosomes along DNAs [26] in very good agreement with the experimental evidence.

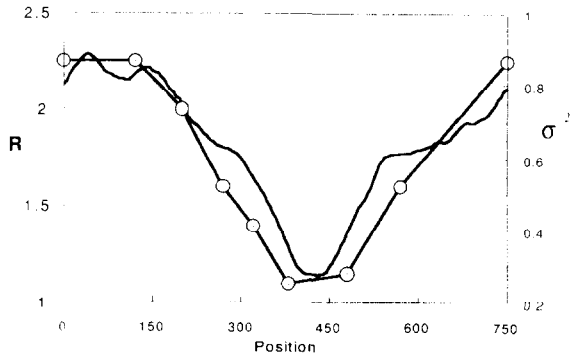

Fig. 6. Comparison between the theoretical (σ^2) and the experimental cyclic permutation gel electrophoresis retardation trend of the 1509–2261 SV40 DNA tract. The experimental data are those reported in Ref. [39].

In addition the distortion energy has been evaluated in kcal per nucleosome starting from a value of the bending constant deduced from that of the persistence length of a standard DNA chain $P = 500$ Å.

Since $P = 2r/ < \delta^2 >$ and the average deformation energy at room temperature, $f < \delta^2 > /2 = RT$ (adopting the harmonic approximation), the bending constant f can be evaluated as $f = RT\,P/r$. Then, at room temperature, the deformation energy constant can be obtained equal to $2.64 \cdot 10^{-2}$ in kcal/bp degrees^{-2} units. Therefore, the distortion energy of a straight DNA tract to the nucleosomal structure can be evaluated as 36.4 kcal/nucleosome, corresponding to an average bending of 4.4 degrees per bp. This energy was assumed as the origin of the distortion energy diagrams. Curved DNA in phase with the nucleosomal structure is characterized by a distortion energy of several kcals per nucleosome lower as shown in the two cases reported below.

Fig. 7 illustrates the case of 5S ribosomal DNA of *Xenopus*, where a nucleosome was precisely localized in vitro by Rhodes [27]. The distortion energy profile when the histone octamer dyad axis moves following the narrow groove is reported along the 5S rDNA sequence. The periodical pattern represents the phasing between the intrinsic and induced curvatures. The minima indicate the translational positioning of the virtual nucleosome dyad axis. The deepest minimum at the transcription origin corresponds to the experimental positioning even if the almost equivalent minima with the same phase at sequence numbers 10 and 20 could explain the experimental data.

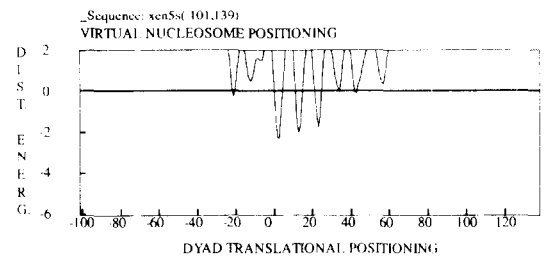

Fig. 7. Distortion energy diagram of *Xenopus* 5S ribosomal DNA. The energy is given in kcal/nucleosome with respect to that of a straight DNA. The minima map the virtual positions of the nucleosome dyad axis along the sequence. Energy values greater than 2 kcal/nucleosome are cut off.

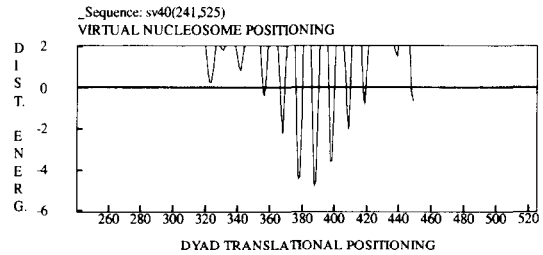

Fig. 8. Distortion energy diagram of a DNA tract near to hypersensitive region in SV40. The energy is given in kcal/nucleosome with respect to that of straight DNA. The minima map the virtual positions of the nucleosome dyad axis along the sequence. Energy values greater than 2 kcal/nucleosome are cut off.

The theoretical nucleosome positioning near the hypersensitive region (280–525) in SV40 is shown in Fig. 8: the deepest minimum corresponds exactly to the experimental localization obtained with a uncertainty of 3 bp by Powers and Bina [28].

The same good agreement we obtained in predicting histone octamer binding sites on the regulatory region (−300 to 600) of SV40 chromatin investigated by Ambrose et al. by cloning and sequencing nucleosomal DNAs obtained from micrococcal nuclease digestion of chromatin [26,29].

5. Conclusions

The conclusions reached in the present paper, to which we arrived by using our previously introduced mathematical treatments, prove the general feasibility of DNA curvature studies based on our as well as on other static models proposed by different authors; it is worth to remember the model devised by Calladine et al. based on X-ray data and steric considerations [30–34], or the last model introduced by Trifonov which adopts an empirical matrix of wedge angles obtained by fitting electrophoretic data [35–37] and finally the model employed by Crothers [38] which empirically introduces bends at the hypothetical structural transition between canonical B-DNA and DNA tracts characterized by repeated AA sequences.

In fact, all these models although based on static models of DNA curvature show a satisfactory agreement with experimental data.

We suggest that the time average curvature parameters of a DNA tract represented by the static (thermodynamic) model, is useful to study physical and biological events characterized by correlation times significantly higher than that of the dynamic fluctuations. The dynamic model, however, is more realistic for faster events and could be more useful for long tracts of DNA.

Acknowledgements

We thank D. Rhodes for useful discussions.

This research was supported in part by CNR 'Progetto Finalizzato Chimica Fine'.

Appendix 1

Derivation and properties of the complex-plane representation of the DNA curvature

The curvature vector

The DNA curvature $c(n)$ is a local property of the B-DNA axis and represents its directional change along the sequence. It is defined as having a modulus equal to the reciprocal of the curvature radius of the writhing B-DNA axis assuming the average length of a turn of the double helix as unitary step. This quantity can be calculated following the Cambridge convention (see Fig. 9) by transforming the coordinate system fixed at the first base pair average plane of the chain as in B-DNA (with the z axis in the

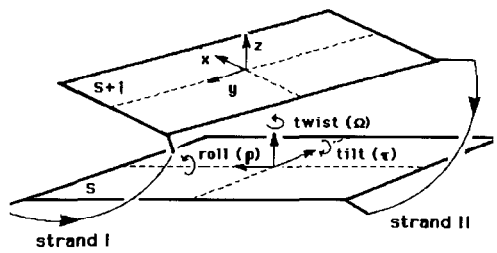

Fig. 9. Orientational parameters of the base pair average plane in a dinucleotide step.

positive direction of the helical axis and the x axis along the pseudo dyad axis of the base pair and pointing towards the large groove), equivalently fixed at the first base pair of the next turn of double helix.

If $\mathbf{A}_s = \Omega_s \mathbf{R}_s \mathbf{T}_s$ represents the transformation matrix of a coordinate system at $(s-1)$ in that of sequence number s, corresponding to the product of the rotation matrices of argument Ω_s (the twist angle around z axis), ρ_s (the roll angle around y axis) and τ_s (the tilt angle around x axis), the change in direction of the B-DNA axis after one nucleotide step is represented by the vector:

$$(\mathbf{A}_s^+ - \mathbf{U}) \begin{vmatrix} 0 \\ 0 \\ 1 \end{vmatrix} \tag{1}$$

($\mathbf{U}$ is the unit matrix).

Thus, the change in the helical axis direction between the sequence number n_1 and n_2 is given by:

$$\left[\left(\prod_{s=n_1}^{n_2} \mathbf{A}_s^+ \right) - \mathbf{U} \right] \begin{vmatrix} 0 \\ 0 \\ 1 \end{vmatrix} \tag{2}$$

The slight values of ρ and τ allow the reduction of the matrices involved at the first order of Taylor series. Thus, Eqs. (1) and (2) become respectively:

$$\begin{vmatrix} \Omega_S^+ - \mathbf{U} \\ -(\Omega_S \mathbf{d}_S)^+ \end{vmatrix} \begin{vmatrix} \mathbf{d}_S \\ -\frac{|\mathbf{d}_S|^2}{2} \end{vmatrix} \begin{vmatrix} 0 \\ 1 \end{vmatrix} = \begin{vmatrix} \mathbf{d}_S \\ -\frac{|\mathbf{d}_S|^2}{2} \end{vmatrix} \tag{3}$$

the superscript$^+$ indicates the transpose matrix and

$$\begin{vmatrix} \prod_{s=n_1}^{n_2} \Omega_s^+ - \mathbf{U} \\ -\left[\prod_{s=n_1}^{n_2} \Omega_s \mathbf{c}_n \right]^+ \end{vmatrix} \begin{vmatrix} \mathbf{c}_n \\ -\frac{|\mathbf{c}_n|^2}{2} \end{vmatrix} \begin{vmatrix} 0 \\ 1 \end{vmatrix} = \begin{vmatrix} \mathbf{c}_n \\ -\frac{|\mathbf{c}_n|^2}{2} \end{vmatrix}$$

in supermatrix form:

$$\Omega_s^+ = \begin{vmatrix} \cos \Omega_s & -\sin \Omega_s \\ \sin \Omega_s & \cos \Omega_s \end{vmatrix}; \mathbf{d}_s = \begin{vmatrix} \rho_s \\ -\tau_s \end{vmatrix}$$

The curvature vector is defined in the plane perpendicular to the helical axis as:

$$\mathbf{c}_n = \mathbf{d}_{n_1} + \Omega_{n_1}^+ \mathbf{d}_{n_1+1} + \ldots + \prod_{s=n_1}^{n_2-1} \Omega_s^+ \mathbf{d}_{n_2}$$

and assigned to the central nucleotide of the tract considered:

$$n = \frac{n_1 + n_2}{2}$$

The deviation vector, $\mathbf{d}_s$, and the curvature vector, $\mathbf{c}_n$, lie in the xy plane. This reduction is a very good approximation because the intrinsic curvature is generally less than $20°-25°$ per turn and $\mathbf{c}_n$ is actually approximated at the second order of Taylor series because the first terms which were not considered contain triple products of roll and tilt angles.

The curvature vector of DNA is conveniently calculated as a vectorial summation in the complex plane by changing the x and y axis in the real and imaginary axes, respectively, and adopting an average value for Ω_s $(2\pi/\nu)$ corresponding to the periodicity of B-DNA, ν, in the tract considered.

In this representation:

$$\mathbf{d}_s \equiv \mathrm{d}(s) = \rho_s - i\tau_s$$

and

$$\mathbf{c}_n \equiv c(n) = \frac{\nu}{n_2 - n_1} \sum_{s=n_1}^{n_2} \mathrm{d}(s) \exp(2\pi i s/\nu)$$

A useful representation of the distortions of B-DNA axis along the chain is given by the 'curvature diagram' which gives the value of curvature per turn $c(n)$ in modulus and phase calculated for recurrent turns along the sequence, and assuming $\nu = 10.4$ as the average periodicity of the double helix. In this case $n_2 - n_1 = 10$. Thus in general:

$$c(n) = \sum_{n\text{th turn}} \mathrm{d}(s) \exp(2\pi i s/\nu)$$

In this case of summations over nearly a complete turn of B-DNA helix, $c(n)$ is different from zero only when the distribution of d_s contains a harmonic component of frequency ν. It is worthwhile to note that this symmetry feature holds independently from the approximation adopted, also when $c(n)$ is calculated by the standard matrix transformations.

It is interesting to note the logically expected invariance of the curvature to the interchange of the sequence considered with that of the other strand in the correct 5′–3′ direction, because the symmetry properties of the deviation vectors; it corresponds to change $d(s)$ with the complex conjugate $d(s)^*$ and

the sequence number s with $N-s$ in the $c(n)$ formula (N is the total number of bp); so that the curvature of the a strand is the complex conjugate of the curvature of the other strand times a phase factor $\exp(2\pi N/\nu)$.

A more direct derivation of the complex plane representation springs out from the consideration that the vectorial chain of the local deviation vectors rotated of the pertinent phase angle $2\pi/\nu$ of B-DNA helix in the complex plane, corresponding to the vectorial chain on the unit sphere of the directional changes of the local helical axes.

Starting from the curvature diagrams it is possible to reproduce the 3-dimensional superstructure of DNA tracts with a very good approximation, using the product of the pairs of rotation matrices $\mathbf{c}(n)\Phi(n)$ where $\mathbf{c}(n)$ represents the pure rotation around the x axis of an angle equal to the curvature at the sequence number n, and $\Phi(n)$, the pure rotation matrix around the z axis of the difference in phase of the curvature vectors at n and $n+1$ sequence numbers $\phi(n) = \mathrm{tg}^{-1}(\mathrm{Im}(c(n))/\mathrm{Re}(c(n)))$.

The structure obtained is practically identical to that calculated via standard matrix transformations and mathematically coincident in the case of planar curvature [18].

The curvature dispersion

It is interesting to evaluate the central angular dispersion of the directions of the local helical axes on a DNA tract: $\sigma^2 = <C(n)IC(n)> - |<C(n)>I^2$ (the average values are calculated over the N bp DNA tract examined).

This value represents the snaking of DNA chain about its average direction.

Here $C(n)$ represents the integral curvature, namely the deviation vector of the nth local helical axis with respect to the first one.

It can be evaluated using the complex plane representation:

$$C(n) = \sum_{s=1}^{n} \mathrm{d}(s)\exp(2\pi is/\nu),$$

only in the case of DNA tracts characterized by small curvatures or in the case of planar or quasi planar curvature; the approximation becomes progressively worse with the increasing of the curvature out of plane.

In this case σ^2 can be correctly calculated using standard matrix transformations and evaluating the gyration radius on the unit sphere of the chain of the vectorial spherical arcs representing the sequence of angular deviations of the helical axis along DNA.

We call such angular dispersion of the writhing helical axis the 'static curvature dispersion'.

Adopting the same mathematical method it is possible to evaluate the 'dynamic curvature dispersion' of the helical axis under thermal fluctuations as illustrated in the paper.

References

[1] J. Griffith, M. Bleyman, C.A. Rauch, P.A. Kitchin and P.T. Englund, Cell, 46 (1986) 717.
[2] C.H. Hsieh and J.D. Griffith, Cell, 52 (1988) 535.
[3] G. Muzard, B. Théveny and B. Revét, EMBO J., 9 (1990) 1289.
[4] J.C. Marini, P.N. Effron, T.C. Goodman, C.K. Singleton, R.D. Wells, R.M. Wartell and P.T. Englund, J. Biol. Chem., 259 (1984) 8974.
[5] H.M. Wu and D.M. Crothers, Nature (London), 308 (1984) 509.
[6] P.J. Hagerman, Biochemistry, 24 (1985) 7033.
[7] S. Diekmann, FEBS Lett., 195 (1986) 53.
[8] H.S. Koo and D.M. Crothers, Nature (London), 320 (1986) 501.
[9] I.E. Ulanovsky, M. Bodner, E.N. Trifonov and M. Choder, Proc. Natl. Acad. Sci. USA, 83 (1986) 862.
[10] P. De Santis, S. Morosetti, A. Palleschi and M. Savino, Structures and superstructures in periodical polynucleotides, in Clementi and Chin (Editors), Structure and Dynamics of Nucleic Acids, Proteins and Membranes, New York, 1986, p. 31.
[11] P. De Santis, A. Palleschi, M. Savino and A. Scipioni, Biophys. Chem., 32 (1988) 305.
[12] P. De Santis, G. Gallo, A. Palleschi, M. Savino and A. Scipioni, J. Mol. Liq., 41 (1989) 291.
[13] P. De Santis, A. Palleschi, A. Scipioni and M. Savino, Biophys. Chem., 42 (1992) 147.
[14] P. De Santis, A. Palleschi and M. Savino, Electrophoresis, 14 (1993) 699.
[15] D. Boffelli, P. De Santis, A. Palleschi, A. Scipioni and M. Savino, Int. J. Quantum Chem., 42 (1992) 1409.
[16] W.K. Olson, N.L. Marky, R.L. Jernigan and V.B. Zhurkin, J. Mol. Biol., 232 (1993) 530.
[17] D.L. Milton, M.L. Casper and R.F. Gesteland, J. Mol. Biol., 213 (1990) 135.
[18] P. De Santis, A. Palleschi, M. Savino and A. Scipioni, Biochemistry, 29 (1990) 9269.

[19] Y.H. Wang, M.T. Howard and J.D. Griffith, Biochemistry, 30 (1991) 5443.
[20] P.G. De Gennes, J. Chem. Phys., 55 (1971) 572.
[21] L.S. Lerman and H.L. Frisch, Biopolymers, 21 (1982) 995.
[22] O.J. Lumpkin and B.H. Zimm, Biopolymers, 21 (1982) 2315.
[23] B.H. Zimm and S.D. Levene, Q. Rev. Biophys., 25 (1992) 171.
[24] N.L. Marky and W.K. Olson, Biopolymers, 34 (1994) 121.
[25] H.R. Drew and A.A. Travers, J. Mol. Biol., 186 (1985) 773.
[26] P. De Santis, M. Fuà, A. Palleschi and M. Savino, Biophys. Chem., 46 (1993) 193.
[27] D. Rhodes, EMBO J., 4 (1985) 3473.
[28] J.H. Powers and M. Bina, J. Mol. Biol., 221 (1991) 795.
[29] C. Ambrose, A. Rajadhyaksha, H. Lowman and M. Bina, J. Mol. Biol., 209 (1989) 255.
[30] C.R. Calladine, J. Mol. Biol., 161 (1982) 343.
[31] C.R. Calladine and H.R. Drew., J. Mol. Biol., 178 (1984) 773.
[32] C.R. Calladine and H.R. Drew, J. Mol. Biol., 192 (1986) 907.
[33] Calladine C.R., Drew H.R. and M.J. McCall, J. Mol. Biol., 201 (1988) 127.
[34] C.R. Calladine, C.M. Collis, H.R. Drew and M.R. Mott, J. Mol. Biol., 221 (1991) 981.
[35] E.N. Trifonov, CRC Crit. Rev. Biochem., 16 (1986) 89.
[36] L.E. Ulanovsky and E.N. Trifonov, Nature (London), 326 (1987) 720.
[37] A. Bolshoy, P. McNamara, E. Harrington and E.N. Trifonov, Proc. Natl. Acad. Sci. USA, 88 (1991) 2317.
[38] D.M. Crothers, T.E. Haran and J.G. Nadeau, J. Biol. Chem., 265 (1990) 7093.
[39] D.L. Milton and R.F. Gesteland, Nucl. Acids Res., 16 (1988) 3931.